CARBON COMPOSITE SEISMIC RETROFIT OF REINFORCED CONCRETE COLUMNS WITH CORRODED REINFORCEMENT

Wilkins Aquino, Assistant Professor, Cornell University, Ithaca, NY
Neil M. Hawkins, Professor Emeritus, University of Illinois at Urbana-Champaign

ABSTRACT

This laboratory study concerns the use of carbon composites to restore the seismic effectiveness of corrosion-damaged reinforced concrete bridge columns with inadequate length lap-spliced reinforcement at their base and subjected to severe environmental conditions. Large-diameter reinforced concrete columns were subjected to accelerated corrosion by using external currents, repaired with different layouts of carbon composite material, subjected to multiple freeze-thaw cycles and finally tested to failure under lateral cyclic loading. Bond degradation due to corrosion dictated the resulting loss in ductility and load capacity. Except for one case, all columns retrofitted with carbon composites matched or exceeded the maximum load and ductility capacity of a control column simulating the as-built condition.

INTRODUCTION

Corrosion of reinforcing steel in concrete structures is a significant durability problem, (Aquino 2002; Castel et al. 2000; Chung et al. 2004; Mangat et al. 1999), for bridges and parking garages located in regions where salt is widely used in winter months. Maintenance of corrosion-damaged structures costs the government and private sectors millions of dollars every year. In addition, if the structure is located in a region of high seismic risk the adequacy of the deteriorated structure to withstand the seismic loadings for which it was originally designed is highly questionable, raising additional safety concerns.

A research project was undertaken by the University of Illinois at Urbana-Champaign to address concerns related of the long-term behavior of columns deteriorated by corrosion and retrofitted with carbon fiber reinforced composites (CFRC). The study was sponsored by the Illinois and Federal Departments of Transportation and used materials supplied by Master Builders. The project involved a laboratory study of the effect of freezing environments and seismic actions on corrosion-damaged CFRC retrofitted columns. The laboratory study complemented an on-going field study of the performance of 12 columns retrofitted with CFRC. This paper concerns the effectiveness of using CFRC to restore the seismic structural capacity of corrosion damaged-columns. The work related to freeze-thaw durability of the repaired columns is reported elsewhere, (Aquino, 2002).

BACKGROUND

Advanced composite materials (ACM) have considerable potential for the repair of reinforced concrete structures damaged by corrosion, (Aquino 2002; Debaiky et al. 2002; Lee et al. 2000; Masoud and Soudki 2001; Soudki and Sherwood 2000; Pantazopoulou et al. 2001; Tastani and Pantazopoulou 2004). Although ACM have been widely accepted for the seismic retrofit of reinforced concrete structures, their use in repairing corroded structures has received less attention. ACM can be a viable alternative to steel jackets for the repair of corrosion-damaged reinforced concrete structures. Lee et al. (2000) studied the response of reinforced concrete

columns with corroding reinforcement and repaired using carbon fiber reinforced composite (CFRC) wraps. Corroded columns without wraps showed moderate decreases in ultimate axial loads and marked reductions in ultimate axial displacements compared to non-corroded control samples. Columns corroded and repaired with CFRC showed significant increases in ultimate load and ductility compared to control specimens. Pantazopoulou et al. (2001) used small-scale specimens to study the effectiveness of ACM in upgrading the response of corrosion-damaged axially loaded columns. Columns repaired without removing damaged concrete before the application of the ACM performed better than the columns where damaged concrete was first replaced with a repair grout. Tastani and Pantazopoulou (2004) used half-scale specimens to examine the structural behavior of corrosion-damaged columns with reinforcement details representative of pre-1980 Codes. Columns were upgraded using glass and CFRC wraps after being conditioned using accelerated electrochemical corrosion. After upgrading specimens were tested to failure under axial compression. The best performance was for specimens with cover replacement by high strength grout prior to wrapping. With CFRC wraps failures were rather brittle with axial strains at peak loads and at failure being similar and ranging between 0.005 and 0.015 depending on jacket details.

Masoud and Soudki (2001) tested reinforced concrete beams deteriorated by corrosion, repaired with CFRC, and subjected to monotonic and fatigue loading. CFRC significantly improved the mechanical response of beams deteriorated by corrosion. Soudki and Sherwood (2000) investigated the effect of corrosion on reinforced concrete beams already strengthened with CFRC. They found that ultimate strength, yield strength, and stiffness decreased with increasing levels of corrosion in all their specimens. However, reduction in load and deformation capacity was less pronounced in members strengthened using CFRC. Chung et al. (2004) electrochemically corroded the reinforcement in slabs to between 85 and 99% of its original cross-sectional area and then tested the slabs to failure under four point bending. Starting from the 2% corrosion level there was an increasing effect of corrosion level on bond strength and development length.

EXPERIMENTAL PROGRAM

Six identical reinforced concrete columns 500 mm (20 in) in diameter and 2450 mm (96 in) in height were built in the laboratory. Specimens were 1/3-scale models of field columns located in East St. Louis, IL. Laboratory specimen details are shown in Fig.1. The columns were reinforced longitudinally with 12 #8 steel bars that were spliced to 8 #8 steel bars protruding as dowel bars from a square base. The 750 mm (30 in) extension of the dowel bars above the foundation beam duplicated the 30 bar diameter extension of the same bars in the field columns. In regions of high seismic risk current codes require 40 bar diameter extensions and the aim of this investigation was to see if CFRC retrofits could simultaneously address both corrosion and seismic inadequacies of existing construction. Column lateral reinforcement consisted as #3 steel circular hoops spaced 200 mm (8 in) on centers.

The column concrete compressive strength was 32 MPa (4600 psi) at 28 days. All reinforcing bars were Grade 60 steel. The concrete mix had an air content equal to 5% to provide for resisting severe freezing and thawing conditions. The CFRC system used for retrofitting the columns consisted of unidirectional carbon fiber sheets and an epoxy resin. The carbon fiber sheets had a thickness of 0.63 mm (0.025 in) and contained a fiber volume fraction of

approximately 26%. The properties of the carbon fiber reinforced plastic (CFRP), as reported by the manufacturer, are given in Table 1.

Five columns were subjected to accelerated corrosion by using external currents and one was kept in the as-built condition as a control column. Four of the five deteriorated specimens were repaired using CFRC and one column was kept in the deteriorated state for comparison purposes. The research program also included the study of the effects of freeze and thaw on the CFRP repaired columns. The structural responses of the repaired columns were not affected by freezing and thawing damage. Aquino (2002) provides further details on the freeze and thaw experiments.

Corrosion Process. External current was used to induce corrosion in the columns. A parallel circuit arrangement was used as shown in Figure 3. Although a series circuit arrangement is preferable for achieving the same level of corrosion in all specimens in a given amount of time, a parallel arrangement was used to reduce the voltage needed to induce the current demand required for these large-scale specimens.

The work of Mangat and Elgarf (1999) was used to estimate the degree of corrosion and the corrosion rate. The degree of corrosion is defined here as the reduction in bar diameter expressed as a percentage of the original bar diameter. A degree of corrosion equal to 4% was selected for these experiments because, based on Mangat and Elgarf's results, that corrosion level results in significant loss of capacity. The realism of that degree is confirmed by Chung et al.'s results. The rate of corrosion selected was 0.25 mA/cm^2 in order that the desired degree of corrosion was achieved in a reasonable length of time.

To duplicate the type of corrosion observed in the field, only part of the column needed to be corroded. Further, for seismic actions the response of a pier causes maximum moment at the column base where moments must be resisted by dowel reinforcement. Hence, the column section selected for corrosion extended from its base (top of the foundation beam) to a distance of 450 mm (18 in) above the top of the lap splice for a total corroded length of 1200 mm (48 in).

Copper mesh placed around the perimeter of each column was used as external cathode. A 3% sodium chloride solution was used as electrolyte to conduct the ionic current from the anode (steel reinforcement) to the cathode (copper mesh), while high-density polyethylene pipes were used to store the saline solution around the corroding columns. The current and voltage in each column were measured periodically and areas under the current–time plots for specimens made similar. From Faraday's law, the mass loss is directly proportional to the area under the current-time plot. Hence, equal current-time plot areas represent equal total mass loss.

At termination of the corrosion process no spalling of the concrete cover had occurred. However, the level of corrosion in terms of width and extent of splitting cracks, and of corrosion products, duplicated the extant conditions for many field columns.

Repair Process. The repair process consisted of removing deteriorated concrete to a depth of 25 mm (1 in) beyond the dowel bars, cleaning the corroded reinforcing steel, casting repair material, and wrapping the columns using CFRP. Due to the confinement provided by the composite wraps, it was not considered necessary to replace deteriorated hoop bars many of which had corrosion fractures. The repair material was a normal strength concrete with a 28-day

compressive strength of MPa (5000 psi). Wraps were installed on the columns after allowing the repair concrete to cure for a minimum of 14 days.

In order to study the effects of freezing and thawing and moisture encapsulation on the performance of the retrofitted columns, different layouts of CFRP bands were used for wrapping the columns. The number of carbon composite layers used was determined by following the procedure developed previously for upgrading columns with inadequate lap-splices (Hawkins et al., 2000). The wraps were designed to provide the same level of confinement for all columns.

Loading frame, instrumentation, and data acquisition. Figure 3 shows the loading frame and instrumentation used for the lateral load tests. Each column was cast with a square base that, for structural testing, was grouted into the central opening of a foundation beam bolted to the laboratory floor. The foundation beam was then post-tensioned in two directions to minimize cracking during testing.

Lateral deflections at the top of columns, rotations at the base, strains in the reinforcing steel, and circumferential strains in the wraps were continuously recorded during each test. Deformations in the grouting material filling the space between the column and the base beam gave rise to rigid body motions in the column during loading. Those motions were measured using cable extension transducers and linear variable differential transformers (LVDT).

Load history. The same incremental displacement loading history was used for all columns. Three full cycles were applied at each displacement, using a triangular waveform. The initial displacement corresponded to 1/8 of the anticipated yield displacement, Δ_y, and subsequent displacements were increased every three cycles to 0.25 Δ_y, 0.5 Δ_y, 0.75 Δ_y, Δ_y, 1.5 Δ_y, 2.5 Δ_y, 3.5 Δ_y, etc. until the column failed or the maximum displacement of the actuator was reached. Failure was declared if the peak load during a given set of three cycles dropped to eighty five percent of the absolute maximum load attained during the previous set of three cycles.

TEST RESULTS

Visual assessment of corrosion-damaged columns. Figure 4 shows the appearance of the columns at the end of the corrosion process. In every case vertical cracks formed on the column surfaces along the lines of the longitudinal reinforcing bars. In some cases horizontal cracks also delineated the positions of the lateral steel hoops. The amounts of dark corrosion products deposited on column surfaces varied noticeably from specimen to specimen, despite each specimen having been subjected to the same corrosion level.

For repair, the reinforcement in the columns was exposed and a visual assessment was made of the uniformity and extent of corrosion damage. The amount of reinforcing steel deterioration was similar in all columns. Column bar material losses were concentrated on the parts of their surfaces closest to the exterior of the column. Dowel bars showed far less corrosion damage than column bars. This result was expected because dowel bars were not connected directly to the circuit and could interact electrically with column bars only through metal spacers left during construction and through the lateral steel hoops. In every column, the lateral steel hoops were severely damaged with entire cross sections lost at localized points in several cases.

Lateral cyclic load results. Table 2 summarizes the tests results. The main parameters studied in this investigation were yield loads, Fy, ultimate loads, Fu, displacements at yield load, Δ_y, displacements at maximum load, Δ_u , axial strains in the reinforcing steel, circumferential strains in the composite wraps, and rotations at the base of the column. The yield load and displacement were taken as the point at which the load-displacement curve departed from essentially linear elastic behavior. The ductility ratio at maximum load, μ, was computed as Δ_u/Δ.

Column 6 – Control Column. Figure 5(a)[1] shows the load-deformation response of control Column 6. The response of the column was characterized by stable hysteretic loops for both directions of loading. The column achieved a displacement ductility ratio of approximately 4. Several small horizontal flexural cracks were observed prior to the yield load. However, major cracks running parallel to the longitudinal reinforcement formed as the maximum load was approached and they opened significantly shortly after the maximum. The pattern of cracking was typical of that for columns with bond failures due to inadequate splice lengths.

Column 4- Unrepaired Corroded Column. Figure 5(b) shows the load-displacement response. The hysteretic behavior was stable up to a load of 133 kN (30 kip) and a maximum displacement of 21 mm (0.8 in). Subsequent cycles to the same displacement resulted in a marked decrease in load capacity in the positive direction, while capacity in the negative direction remained unchanged. At that peak displacement corrosion cracks parallel to the column steel opened significantly. The column was declared to have failed in spite of the residual capacity for one direction of loading.

Because the load in the negative direction could still be increased, the residual capacity of the column for that loading direction was investigated. Additional displacement increments were applied according to the standard load history, but in the negative direction only. Figure 5(c) shows a load-deformation plot for the full loading history of the column. A clear yield plateau occurred for the negative half of the load-deformation plot at a load of 142 kN (32 kip) and a displacement of 25 mm (1 in.). The maximum load was 150 kN (34 kip) at a displacement of 58 mm (2.3 in). Failure during cycling in the negative direction occurred due to rupture of the deteriorated lateral hoops and subsequent buckling of the column bars.

Column 2 – Retrofitted with 75 mm Bands. The load-displacement plot for this column is shown in Figure 5(d). Well-defined yielding and stable hysteretic loops in both directions of loading characterized its behavior. The maximum load was 169 kN (38 kip) and the corresponding displacement and displacement ductility ratio were 78 mm (3.1 in) and 3.5, respectively. The hysteretic response of Column 2 shows pinching in the form of strong convexity of the load-deformation curve near the horizontal axis after the yield load was attained. The pinching was attributed to partial bond-slip failure of the dowel bars because rigid body motions between the column and foundation beam as measured by the cable transducers were negligible.

---

[1] The X and Y axes scales in plots of load versus deformation differs from case to case. This was purposely done to accentuate the differences in structural response described in the text.

Load-circumferential strain plots for the FRPC bands are shown on Figure 6(a). As the load increased the load-deformation cycles shift to the right, signaling damage in the concrete enclosed by the composite bands. That increase in circumferential strain was due to volumetric expansion of the concrete caused by its progressive damage. For the compression side the expansion was due to the high longitudinal compressive stresses causing marked lateral expansions, while for the tension side circumferential strains also increased due to concrete splitting caused by mechanical locking of bar lugs with surrounding concrete.

Column 3 – Retrofitted with 150mm Bands. The hysteretic behavior of Column 3, shown in Figure 5(e), was stable for both directions of loading. There was a distinct yield plateau followed by a gradual hardening up to a maximum load, followed by gradual softening after that maximum load. The test was stopped before failure of the column due to extensive damage to the foundation beam. The maximum load for this column was 174 kN (40 kip) and the maximum displacement and displacement ductility ratio were 188 mm (7.5 in) and 9.4, respectively. Little or no hysteretic pinching occurred for this column.

Figure 6(b) shows load-circumferential strain plots for the two lowermost FRPC bands. The strains in the lower band were significantly higher than those in the upper band. The maximum strain measured in the lower band was 0.21%, while that for the upper band was only 0.07%.

Column 5 – Retrofitted with 300 mm Bands. Successful completion of this test was prevented by premature failure of the grouting material used to hold the column in place within the opening in the foundation beam. That failure resulted in excessive rigid body rotations and horizontal displacements. However, useful information was still extractable from the test result. The load-deflection plot for Column 5 is shown in Figure 5(f). Severe pinching occurred at the early stages of the load history. The pinching was caused by the rigid body rotations and it was not possible to determine the yield displacement from the load-deflection plot. However, the gages on the dowel bars showed yielding shortly before the maximum load was achieved. The maximum load was 152 kN (34 kip), a value very close to the yield load measured for Columns 2 and 3.

Figure 6(c) shows the load-circumferential strain plot for the lowermost FRPC band. Strains were small compared to the strains developed at maximum load for Columns 2 and 3. That low strain shows that little damage occurred in the concrete in compression and/or bond-slip before testing stopped. Clearly, the maximum load carrying capacity of this column was not reached, but probably that capacity was comparable to the capacities of Columns 2 and 3.

Column 1 – Retrofitted with Continuous Jacket. The load-deformation plot for Column 1 is shown in Figure 5(g). The hysteretic response was similar for both directions and the column showed stiffness degradation early in its loading history. The response showed no distinctive yield point. Successive load peaks increased following a non-linear trend until a maximum load of 120 kN (27 kip) and a corresponding displacement of 43 mm (1.7 in) were reached. For greater displacements the response showed increasing softening and the test was stopped when the load dropped to 70 kN (15.7 kip). Marked pinching characterized the load-deformation response from early in the loading. The cable transducers attached to the column indicated negligible rigid body translation or rotation during the test. Hence, the pinching was caused mainly by bond-slip failure. The strain gages installed on the reinforcing bars indicated that they did not reach yield, confirming bond-slip problems.

Load-circumferential strain plots for the FRPC jacket are shown in Figure 6(d). Strains started to increase rapidly at the relatively low load of 50 kN (11 kip). A maximum strain of 0.2% was registered by the lower gage and of 0.13% by the upper gage, despite the relatively low load capacity of the column. Again, this result supports the finding of a bond-slip type of failure.

DISCUSSION

Importance of Repair Process. Bond degradation dependent on the extent of corrosion was the primary factor controlling the structural response of the specimens. Figure 7 illustrates conceptually the extent of the damage in the concrete surrounding the column and dowel bars as a result of the corrosion process. Only column bars were directly connected to the external power source so that dowel bars experienced little damage from direct corrosion. However, the load capacity of Column 4 (corroded and not repaired) was 80%, and the maximum displacement was only 25%, of that of the non-corroded control column. Those facts, along with observations of the interior of the specimen after cyclic testing, document that damage in the concrete extended to the exterior surface of the dowel bars, and that therefore there was degradation of the concrete between the dowel and column bars.

The degradation of Column 4 can be explained as follows. During loading, tensile stresses are transferred from dowel bars to column bars through shear stresses in the concrete between bars. Limited capacity exists in corroded columns to carry these shear stresses because of cracking and accumulation of rust products in the concrete between dowel and column bars. Axial stresses in column and dowel bars cause radial stresses in the surrounding concrete due to the interlocking of bar lugs and concrete. Radial stresses widen the existing cracks produced by the build up of corrosion products, resulting in further loss of bond and causing loss of column flexural capacity.

The literature usually reports that accelerated corrosion tests on small specimens result in unrealistic evenly distributions of corrosion products. That was not the case here. Column 4 exhibited a marked unsymmetrical hysteretic load-deformation response, clearly indicating that corrosion damage was unevenly distributed. Because uneven distribution of corrosion products is expected in real-life situations, the results of these experiments probably represent the potential behavior of corroded reinforced concrete columns in the field.

Past work in retrofitting with ACM has concentrated on corroded columns subjected to axial loading or beams subjected to transverse loading only. During pure axial loading of corroded columns, wrapping the columns with ACM increases the axial capacity of the damaged concrete through high confining stresses, as was observed by Lee et al. (2000) and Pantazopolou et al. (2001). However, these results show that if corrosion-damaged columns are repaired using ACM and then subjected to lateral loading, the response mechanisms are distinctively different.

Figure 8 shows the crack-damage pattern for corroded specimens observed in this research. The pattern is consistent with that reported by Lee et al. (2000). Direct installation of ACM on the surface of a corroded column with the crack pattern of Fig. 8 is of little help in improving the structural behavior for lateral loading. Volumetric expansion of the concrete is required before the confinement provided by the ACM is activated, which translates into further opening of existing cracks and, hence, reduced interlock and transfer capacity across the crack surfaces. Damaged concrete must be removed and replaced before a column is wrapped with ACM.

Effectiveness of Wrapping. Columns 1, 2, 3, and 5 were repaired with FRPC. The load capacities of Columns 2 and 3 matched or exceeded the capacity of the control column, Column 6. The ductility of Column 2 was similar to that of Column 1, while the ductility of Column 3 greatly exceeded the ductility of Column 1. Column 5 could not be tested to its full capacity due to the premature failure of the grouting material in the square base. Column 1 developed a bond-slip failure prior to yielding of the reinforcing bars.

Although Columns 2 and 3 both had yield and ultimate load capacities exceeding those of the control Column 6, their ductility capacities differed significantly. Column 2 exhibited marked pinching, signifying bond-slip degradation, shortly after reaching its yield load while Column 3 exhibited little pinching throughout the test. This is a surprising result since repair was performed similarly for both columns. In addition, the FRPC theoretically provided the same degree of confinement for all columns. However, inspection after testing was completed of the repair concrete used in Column 2 revealed poor compaction around the reinforcing steel, providing the reason for the marked pinching observed in its load-displacement response.

Column 1, retrofitted with a continuous jacket, also did not perform as expected, failing at a load and displacement significantly lower than those of the control column. Pinching, as in other cases, was associated with bond-slip failure at the dowel reinforcement. The lack of rigid body motions shown by this column reaffirms the bond-failure hypothesis. In contrast with the behavior shown by Columns 2 and 3, pinching in Column 1 occurred before yielding of the reinforcement, as confirmed from strain measurements during the test. Cross sectional cuts were made after failure of Columns 1 and 3 to visually inspect the concrete. Again it was observed that the concrete was very poorly consolidated around the column and dowel bars in Column 1, while the same concrete in Column 3 was sound and well compacted. The cause of premature failure of Column 1 was poor consolidation of the repair material.

Although Column 5 could not be tested to failure, it was determined that the retrofitting of this column was satisfactory at least with respect to its load capacity. The maximum load measured during the test was 152 kN (34 kip), 8% higher than the yield load recorded for the control column and almost the same level as the yield loads recorded for Columns 2 and 3. Furthermore, the strain gages installed in the composite bands registered low levels of deformations in the ACM, indicating that only limited damage occurred in the concrete. The tests on Columns 1, 2, and 3, show that loss of load and displacement capacity is associated with circumferential strains above 0.1%. The maximum circumferential strain recorded in Column 5 was below 0.025%.

With the retrofitting techniques used in this investigation the structural capacities of corrosion-damaged bridge piers can be restored and possible seismic deficiencies corrected. Based on this research design guidelines can be developed for the retrofitting and seismic upgrading of reinforced concrete members with corroding steel. However, it is imperative that non-destructive testing techniques be used to assess the internal condition of the concrete after the retrofitting is performed as evidenced by the inadequate load-deformation behavior of Columns 1 and 2 due to poor consolidation of the repair concrete.

CONCLUSIONS

This investigation showed that: (1) Advanced composite materials (ACM) are a viable alternative for the repair and seismic upgrading of corroded columns. Columns retrofitted properly with carbon composite (DFRC) wraps had load and ductility capacities matching or exceeding those of an undamaged control specimen; (2) Corrosion that causes as little as a 4% loss of bar material, can cause much larger reductions in load and ductility capacities. Corrosion causes severe degradation of the bond between concrete and bars and for columns that bond is a more significant factor controlling structural performance than loss of bar cross sectional area; (3) External current use is a viable means for inducing corrosion in large-scale laboratory tests.

REFERENCES

1. Aquino, W. (2002). "Long-term performance of seismically rehabilitated corrosion-damaged columns." PhD Thesis, University of Illinois at Urbana-Champaign, Urbana, IL.
2. Castel, A., Francois, R., and Arliguie, G. (2000). "Mechanical behavior of corroded reinforced concrete beams-Part 1: Experimental study of corroded beams." Materials and Structures, V.33, pp. 539-544.
3. Castel A., Francois R., and Arliguie, G. (2000) "Mechanical behavior of corroded reinforced concrete beams-Part 2: Bond and notch effects." Materials and Structures, V.33, pp. 545-551.
4. Chung, L., Cho, S-H., Kim, J-H. J., and Yi, S-T. (2004) " Corrosion factor suggestion for ACI development length provisions based on flexural testing of RC slabs with various levels of corroded reinforcing bars," Engineering Structures, V. 26, July pp. 1013-1026.
5. Debaiky, A. S., Green, M. F., and Hope, B. B. (2002). "Carbon fiber-reinforced polymer wraps for corrosion control and rehabilitation of reinforced concrete columns." ACI Materials Journal, V.99, No.2, pp.129-137.
6. Hawkins, N.M., Gamble, W.L., Shkurti, F.J. and Y. Lin, (2000) "Seismic strengthening of inadequate length lap splices", Proceedings, 12th World Conference on Earthquake Engineering, Auckland, New Zealand.
7. Lee, C., Bonacci, J. F., Thomas, M. D. A., Maalej, M., Khajehour, S., Hearn, N., Pantazopoulou, S., and Sheik, S. (2000). "Accelerated corrosion and repair of reinforced concrete columns using carbon fibre reinforced polymer sheets." Can. J. Civ. Eng., V.27.
8. Mangat, P. S., and Elgarf, M. A. (1999). "Flexural strength of concrete beams with corroding reinforcement." ACI Structural Journal, V.96 No.1, pp.149-158.
9. Masoud, S. G., and Soudki, K. A. (2001). "Rehabilitation of corrosion-damaged RC beams with FRP sheets." FRP Composites in Civil Engineering, Vol. II, J.-G. Teng (Ed.).
10. Pantazopoulou, S. J., Bonacci, J. F., Sheik, S., Thomas, M. D. A., and Hearn, N. (2001). "Repair of corrosion-damaged columns with frp wraps." Journal of Composites for Construction, V.5(1), pp.3-11.
11. Soudki, K. A., and Sherwood, T. G. (2000) "Behavior of reinforced concrete beams strengthened with carbon fibre reinforced polymer laminates subjected to corrosion damage." Can. J. Civ. Eng., V. 27, pp.1005-1010.
12. Tastani, S.P. and Pantazopoulou, S.J. (2004) " Experimental evaluation of FRP jackets in upgrading RC corroded columns with substandard detailing," Engineering Structures, V.26, June, pp. 817-829.

Property	Primer	Saturant	Carbon Fibers
Maximum stress Mpa (ksi)	17 (2.5)	55 (8)	4275 (620)
Stress at yield Mpa (ksi)	14.5 (2.1)	54 (7.8)	N/A
Strain at max. stress	0.4	0.030	0.0155
Strain at yield	0.04	0.025	N/A
Strain at rupture (mm/mm)	0.4	0.035	0.0155
Elastic Modulus MPa (ksi)	715 (104)	3035 (440)	228,000 (33,000)
Poisson's ratio	0.48	0.40	N/A
Design strength MPa (ksi)	N/A	N/A	3790 (550)

Table 1. Mechanical Properties of Composite Material Constituents

Specimen	Description	Fy, kN (kip)	Fu, kN (kip)	Δy, mm (in)	Δu, mm (in)	μ	Mode of failure
Column 1	Continuous FRP	N/A	120 (27)	N/A	43 (1.7)	N/A	Bond slip
Column 2	75 mm bands	154 (34.6)	169 (38)	22 (0.88)	78 (3.1)	3.5	Bond slip
Column 3	150 mm bands	154 (34.6)	174 (39.11)	20 (0.8)	188 (7.5)	9.4	No failure
Column 4	Corroded	N/A	133 (30)	N/A	21 (0.84)	N/A	Bond slip/column bar bar buckling
Column 5	300 mm bands	N/A	152 (34.3)	N/A	N/A	N/A	No failure
Column 6	Control	141 (31.65)	165 (37)	20 (0.80)	87.5 (3.5)	3.97	Bond slip

Table 2. Summary of Test Results

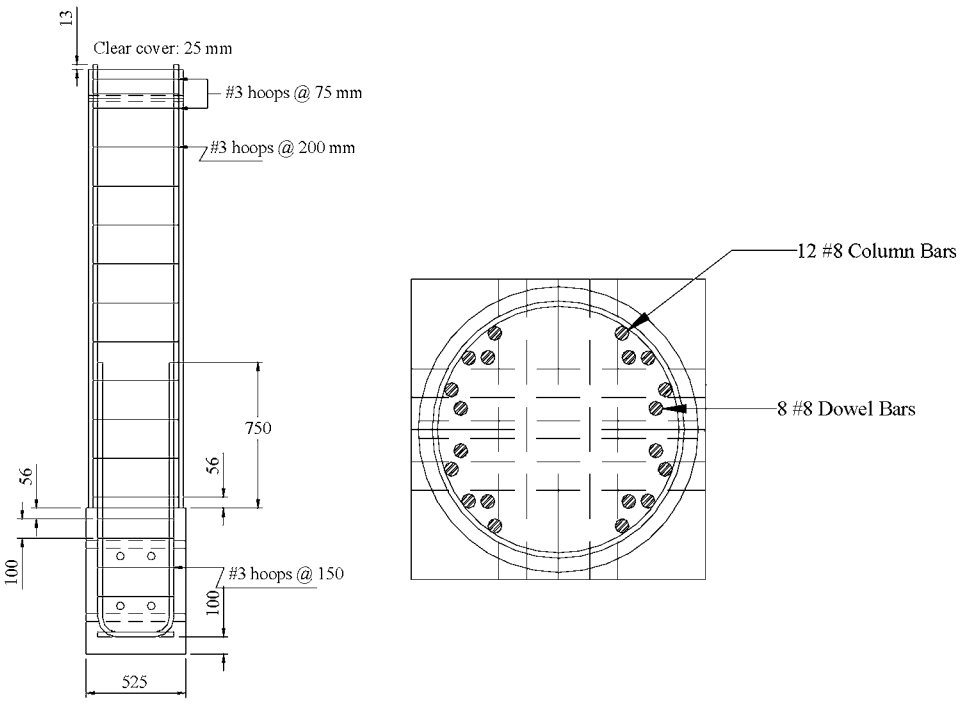

Figure 1. Column Geometry and Reinforcement. Units =mm

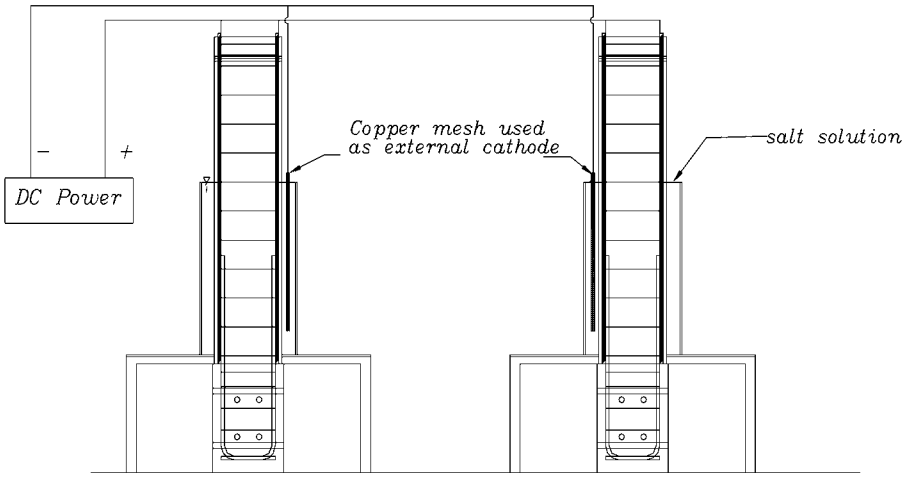

Figure 2. Parallel Circuit Arrangement for Corrosion

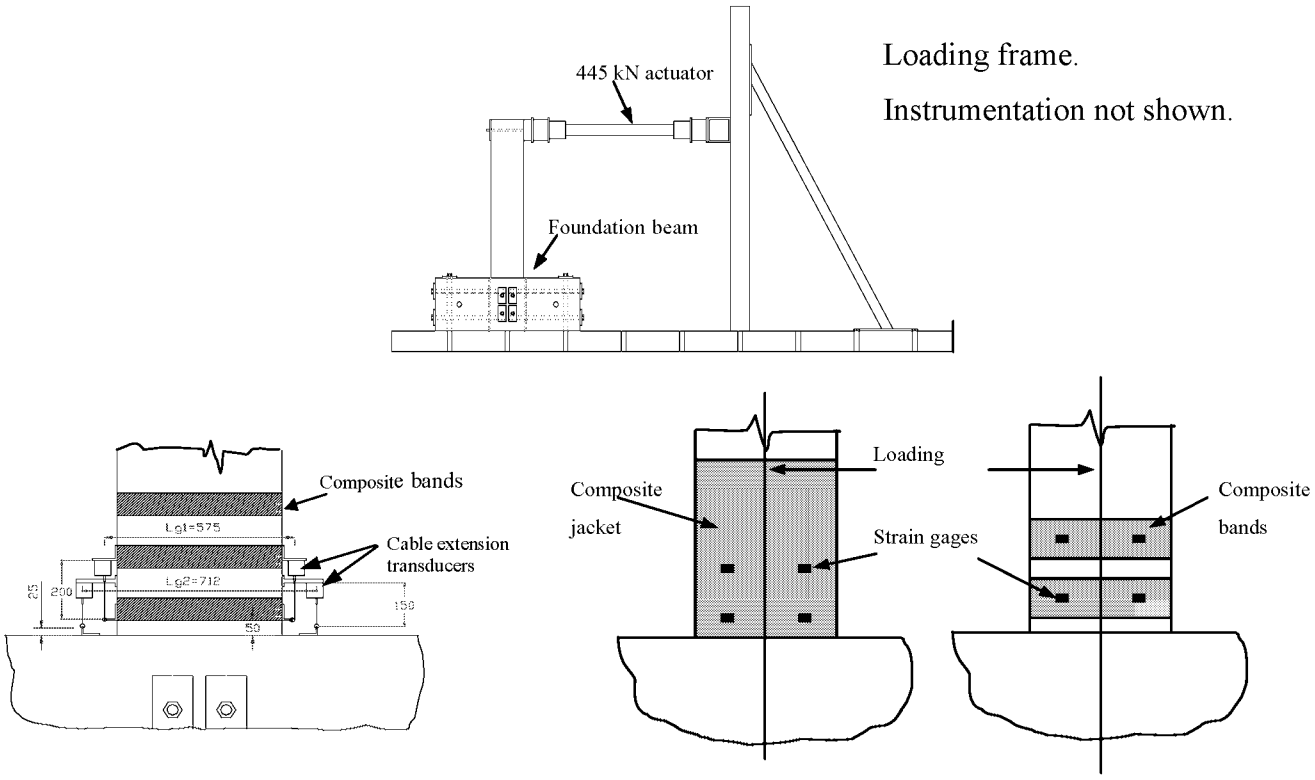

Figure 3. Lateral Load Test Setup. Unit = mm

Column 1 **Column 3** **Column 5**

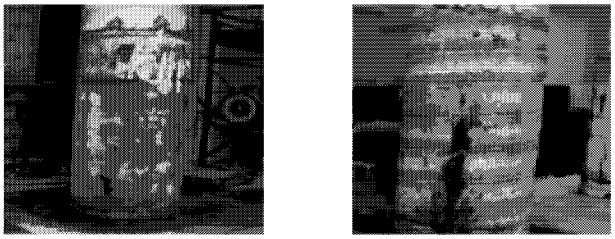

Column 2 **Column 4**

Figure 4. Columns at Completion of Accelerated Corrosion

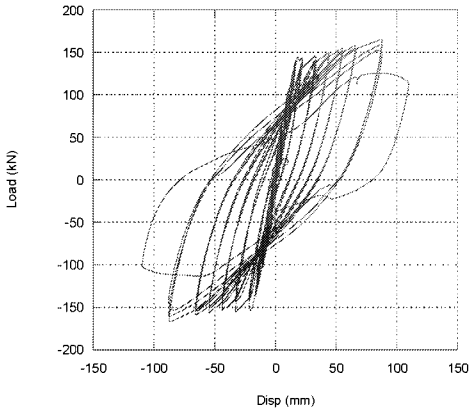

(a) Column 6- Non-Corroded Control

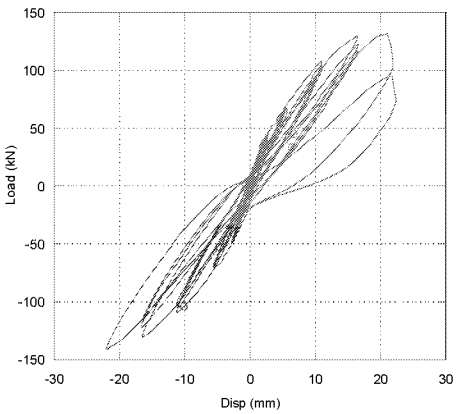

(b) Column 4 –Corroded and Unretrofitted

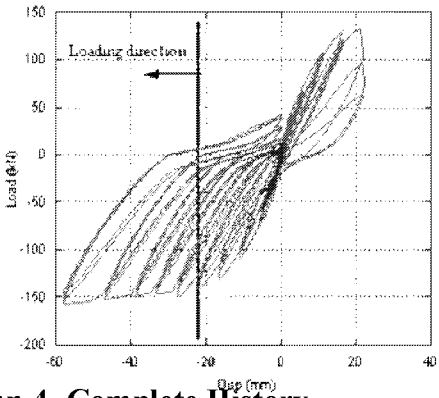

(c) Column 4- Complete History

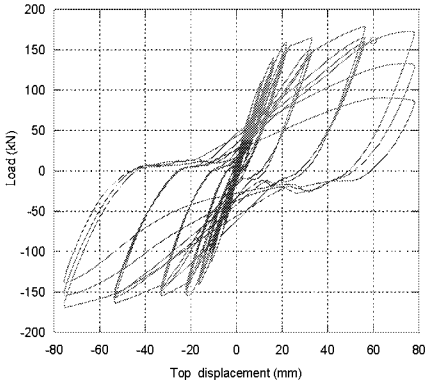

(d) Column2-75mm Bands

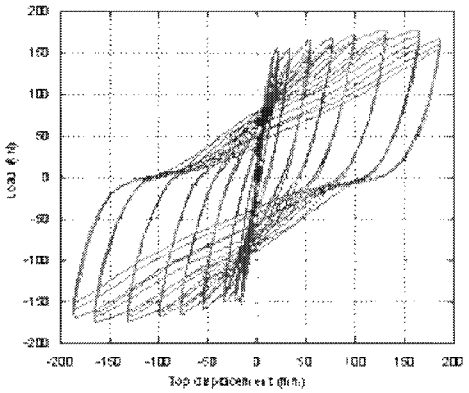

(e) Column 3-150mm Bands

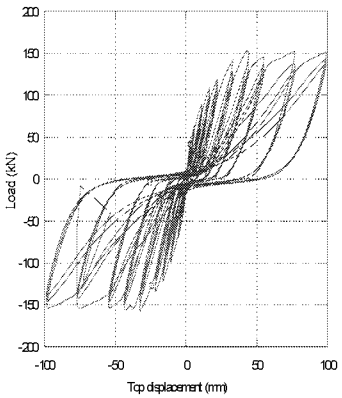

(f) Column 5- 300mm Bands

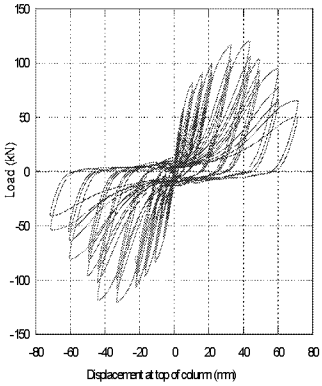

(g) Column 1-Full Jacket

Figure 5. Load-Displacement Hysteretic Behavior

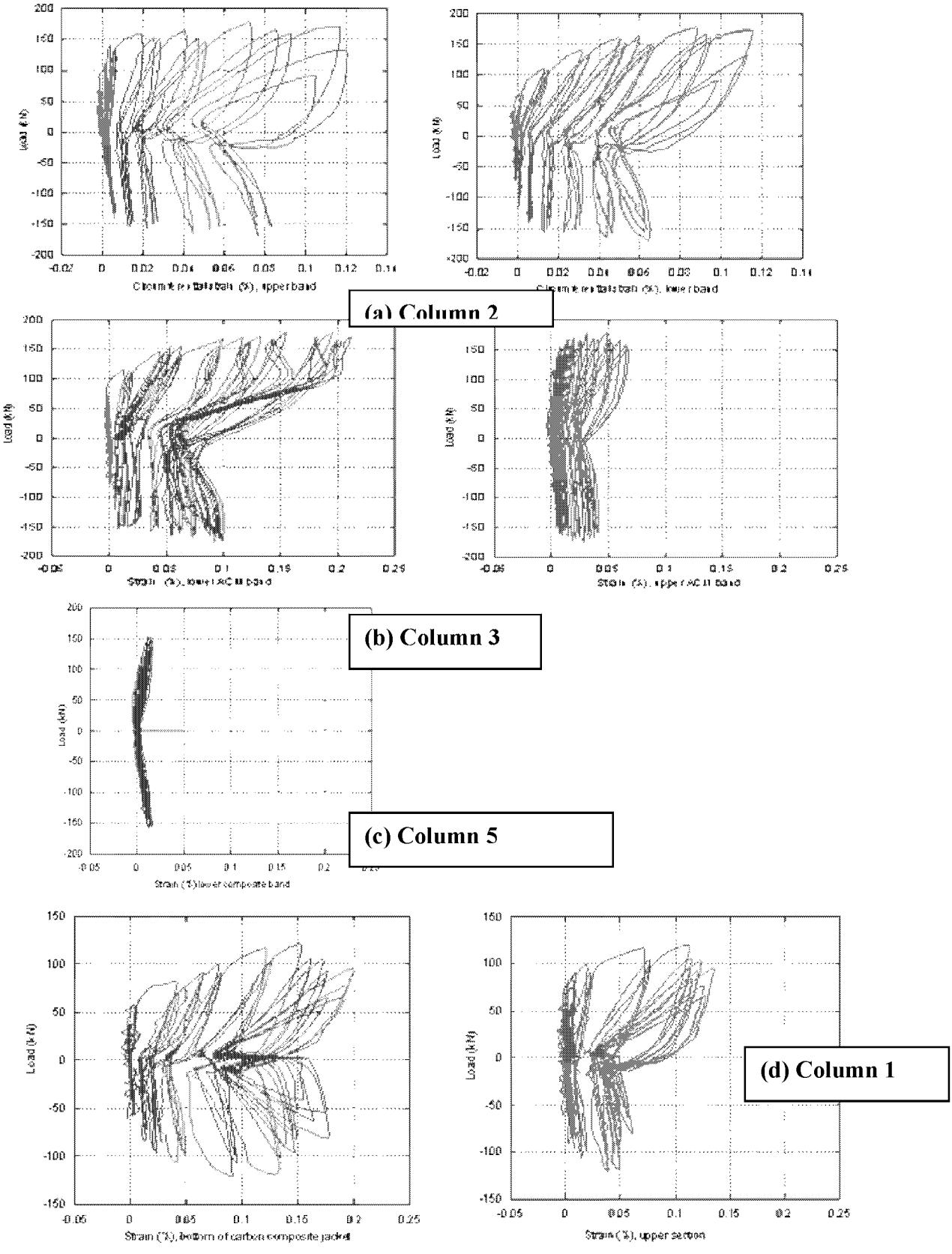

Figure 6. Circumferential Strains in FRPC wraps

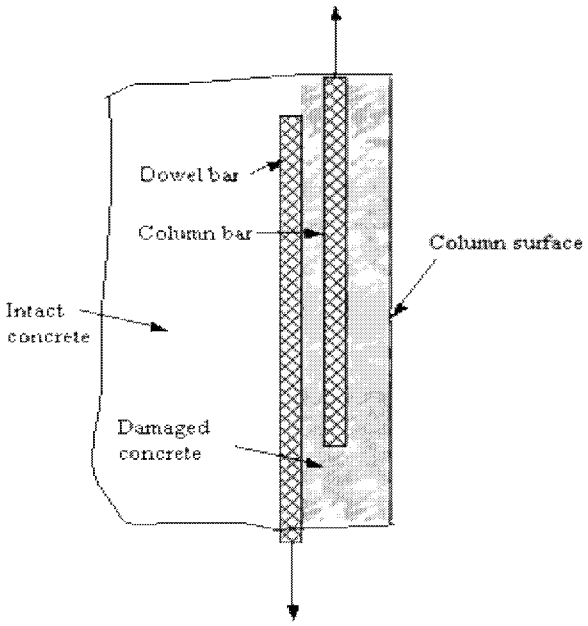

Figure 7. Conceptual Model of Corrosion Damage

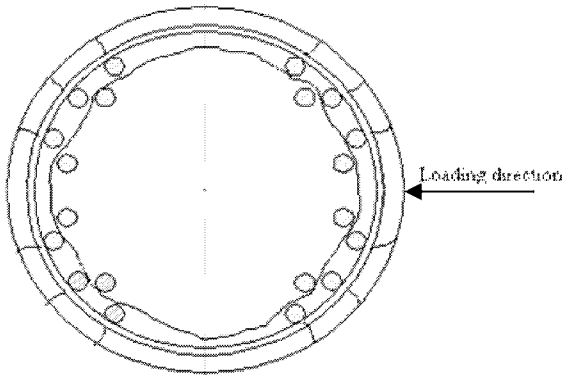

Figure 8. Crack-Damage Pattern After Corrosion